STUK-A231 / NOVEMBER 2008

A

PCXMC

A Monte Carlo program for calculating patient doses in medical x-ray examinations (2nd Ed.)

Tapiovaara M, Siiskonen T

Säteilyturvakeskus
Strålsäkerhetscentralen
Radiation and Nuclear Safety Authority

STUK

STUK

STUK-A231 / NOVEMBER 2008

PCXMC

A Monte Carlo program for calculating patient doses in medical x-ray examinations (2nd Ed.)

Tapiovaara M, Siiskonen T

STUK • **SÄTEILYTURVAKESKUS**
STRÅLSÄKERHETSCENTRALEN
RADIATION AND NUCLEAR SAFETY AUTHORITY

Osoite/Address • Laippatie 4, 00880 Helsinki
Postiosoite/Postal address • PL/P.O.Box 14, FI-00881 Helsinki, FINLAND
Puh./Tel. +358 9 759 881 • Fax +358 9 759 88 500 • www.stuk.fi

The conclusions presented in the STUK report series are those of the authors and do not necessarily represent the official position of STUK

This report is the second revised edition of the report:
Tapiovaara M, Lakkisto M, Servomaa A. PCXMC, a PC-based Monte Carlo program for calculating patient doses in medical x-ray examinations. Report STUK-A139. Helsinki: Finnish Centre for Radiation and Nuclear Safety; 1997.

ISBN 978-952-478-396-5 (print)
ISBN 978-952-478-397-2 (pdf)
ISSN 0781-1705

Edita Prima Oy, Helsinki/Finland, 2008

Sold by:
STUK – Radiation and Nuclear Safety Authority
P.O.Box 14, FI-00881 Helsinki, Finland
Phone: +358 9 759 881
Fax: +358 9 7598 8500

TAPIOVAARA Markku, SIISKONEN Teemu. PCXMC. A Monte Carlo program for calculating patient doses in medical x-ray examinations. STUK-A231. Helsinki 2008, 49 pp.

Key words: PCXMC, x-ray diagnostics, patient dose, effective dose, organ dose, Monte Carlo method, risk assessment, computer program

Summary

PCXMC is a Monte Carlo program for calculating patients' organ doses and effective doses in medical x-ray examinations. The organs and tissues considered in the program are: active bone marrow, adrenals, brain, breasts, colon (upper and lower large intestine), extrathoracic airways, gall bladder, heart, kidneys, liver, lungs, lymph nodes, muscle, oesophagus, oral mucosa, ovaries, pancreas, prostate, salivary glands, skeleton, skin, small intestine, spleen, stomach, testicles, thymus, thyroid, urinary bladder and uterus.

The program calculates the effective dose with both the present tissue weighting factors of ICRP Publication 103 (2007) and the old tissue weighting factors of ICRP Publication 60 (1991). The anatomical data are based on the mathematical hermaphrodite phantom models of Cristy and Eckerman (1987), which describe patients of six different ages: new-born, 1, 5, 10, 15-year-old and adult patients. Some changes are made to these phantoms in order to make them more realistic for external irradiation conditions and to enable the calculation of the effective dose according to the new ICRP Publication 103 tissue weighting factors. The phantom sizes are adjustable to mimic patients of an arbitrary weight and height.

PCXMC allows a free adjustment of the x-ray beam projection and other examination conditions of projection radiography and fluoroscopy. All organ doses calculated by PCXMC are relative to the incident air kerma, $K_{a,i}$. This quantity represents the air kerma at the point where the central axis of the x-ray beam enters the patient. It is given in units of milligray (mGy), free-in-air, without backscatter; see ICRU 74 (2005). The user must supply this datum to the program. The amount of radiation can also be input as the entrance exposure (mR, free-in-air, without backscatter), air kerma-area product or dose-area product (mGy·cm^2), or exposure-area product (R·cm^2). If radiation measurements are not available, the program is able to estimate the incident air kerma also from an input of the x-ray tube current-time product (mAs).

The dose calculation method in PCXMC is the Monte Carlo method. The Monte Carlo calculation of photon transport is based on stochastic mathematical simulation of interactions between photons and matter. Photons are emitted (in a fictitious mathematical sense) from a point source into the solid angle specified by the focal distance and the x-ray field dimensions, and followed while they randomly interact with the phantom according to the probability distributions of the physical processes that they may undergo: photo-electric absorption, coherent (Rayleigh) scattering or incoherent (Compton) scattering. At each interaction point the energy deposition to the organ at that position is calculated and stored for dose calculation. Other interactions are not considered in PCXMC because the maximum photon energy is limited to 150 keV. This chain of interactions forms a so-called history of an individual photon. A large number of independent photon histories is generated, and estimates of the mean values of energy depositions in the various organs of the phantom are used for calculating the doses in these organs.

Calculated organ doses can be used for the assessment of the risk of exposure-induced cancer. The risk estimates are based on the combined absolute and relative risk models of BEIR VII committee (BEIR 2006). PCXMC calculates the risk of exposure-induced death for leukaemia, cancers in colon, stomach, lung, urinary bladder, prostate, uterus, ovaries, breast, liver, thyroid and for all other solid cancers combined. The user may use the risk calculation module for estimating the cancer risk resulting from a single exposure or multiple exposures simulated in PCXMC. The user may also edit the organ doses without calculating doses with PCXMC: a radiation risk assessment can be made for arbitrary irradiation cases.

The present version (2.0) of the program runs in a PC under Windows 95/98/NT/2000/XP/Vista. The Monte Carlo simulation time depends on the desired accuracy and on the speed of the PC, but is typically less than a minute in a PC with a 1.8 GHz processor. The same Monte Carlo data can be used for calculating doses for any x-ray spectrum of interest when the other conditions of the examination remain unchanged; in this case the calculation time is very short because no further Monte Carlo simulations are needed.

The data calculated by PCXMC have been earlier compared to the organ dose conversion factors calculated in NRPB by Jones and Wall (1985) and Hart et al. (1994, 1996) and were found to agree well (Tapiovaara et al. 1997). The excellent agreement with the NRPB data still exists for most irradiation conditions. Small differences are noted in some irradiation conditions, because the composition

and density of the phantom tissues have been changed and the phantoms have been modified from the earlier versions of the program. Reasonable agreement of PCXMC results has also been found in many comparisons with dose measurements and calculations with other phantom models, e.g., Schmidt et al. (2000), Schultz et al. (2003), Helmrot et al. (2007). The usability of the phantom size modification feature of PCXMC has been demonstrated in an extreme case by Smans et al. (2008) who calculated doses in two premature babies with weights of 590 g and 1910 g. The differences between the doses calculated with their voxel phantoms and PCXMC were explained by the differences in the phantom models and the difficulty to place an x-ray field in them in an equivalent fashion. Similar differences between computational and voxel phantoms have also been seen in the papers of Staton et al. (2003), Lee et al. (2006) and Pazik et al. (2007); dose differences of the same order are obtained also in dose calculations with different voxel phantoms (Zankl et al. 2002, Schlattl et al. 2007).

TAPIOVAARA Markku, SIISKONEN Teemu. PCXMC. Monte Carlo -ohjelma röntgentutkimuksista potilaalle aiheutuneiden annosten laskemiseksi. STUK-A231. Helsinki 2008, 49 s. Englanninkielinen.

Avainsanat: PCXMC, röntgendiagnostiikka, potilaan annos, efektiivinen annos, elinannos, Monte Carlo -menetelmä, riskin arviointi, tietokoneohjelma

Tiivistelmä

PCXMC on lääketieteellisistä röntgentutkimuksista potilaille aiheutuneiden elinannosten ja efektiivisen annoksen laskentaan tarkoitettu Monte Carlo -ohjelma. Ohjelmassa tarkasteltuja elimiä ja kudoksia ovat: aivot, aktiivinen luuydin, eturauhanen, haima, iho, imusolmukkeet, kateenkorva, keuhkot, kilpirauhanen, kivekset, kohtu, lihakset, lisämunuaiset, luusto, mahalaukku, maksa, munasarjat, munuaiset, ohutsuoli, paksusuoli, perna, rinnat, rintakehän ulkopuoliset hengitystiet, ruokatorvi, sappirakko, suun limakalvot, sydän, sylkirauhaset ja virtsarakko. Nämä elimet ja kudokset tarvitaan ICRP:n nykyisen määritelmän mukaisen efektiivisen annoksen laskentaan.

Ohjelma laskee efektiivisen annoksen käyttäen sekä nykyisiä kudosten painotuskertoimia, jotka on annettu julkaisussa ICRP Publication 103 (2007), että aikaisempia kudosten painotuskertoimia, jotka on annettu julkaisussa ICRP Publication 60 (1991). Anatominen data perustuu Cristyn and Eckermanin (1987) matemaattisiin, hermafrodiittisiin ihmismalleihin (fantomeihin), jotka kuvaavat kuutta eri-ikäistä ihmistä: vastasyntynyttä, 1-, 5-, 10- ja 15-vuotiaita lapsia ja aikuista. Näihin fantomimalleihin on tehty joitakin muutoksia, jotta ne on saatu paremmin soveltuviksi ulkoisen säteilyaltistuksen arviointitilanteisiin ja jotta efektiivinen annos voitaisiin laskea ICRP 103 -julkaisun mukaisia kudosten painotuskertoimia käyttäen. Fantomien kokoa voidaan säätää, jotta ne saataisiin vastaamaan paremmin eripituisia ja -painoisia potilaita.

PCXMC sallii kuvausprojektioiden ja muiden röntgenkuvaus- ja läpivalaisututkimusten parametrien vapaan käytön laskennassa. PCXMC laskee kaikki elinten annokset suhteessa säteilykeilassa potilaan ihon kohdalla mitattuun ilmakermaan (incident air kerma, $K_{a,i}$). Ohjelman käyttäjän on syötettävä tämä arvo ohjelmaan laskentaa varten: sen syöttäminen voidaan kuitenkin tehdä myös ilmaisemalla käytetyn säteilyn määrä säteilytyksen (X; mR), annoksen ja pinta-alan tulon (DAP; mGy·cm^2) tai säteilytyksen ja pinta-alan tulon (R·cm^2) avulla. Mikäli säteilymittauksia ei ole käytettävissä, ohjelma kykenee arvioimaan kyseisen annoksen ($K_{a,i}$) myös putkivirran ja ajan tulosta (mAs).

PCXMC käyttää laskennassa Monte Carlo -menetelmää, jossa fotonien ja aineen välisiä vuorovaikutuksia simuloidaan stokastisesti. Fotoneita emittoidaan röntgenputken fokuspisteestä avaruuskulmaan, joka määräytyy fokusetäisyyden ja säteilyn kenttäkoon mukaisesti. Fotoneita seurataan, kun ne vuorovaikuttavat fantomissa satunnaisesti niille mahdollisten vuorovaikutusprosessien todennäköisyysjakaumien mukaisesti. Tällaisia vuorovaikutuksia ovat valosähköinen absorptio, koherentti (Rayleigh)sironta ja epäkoherentti (Compton)sironta. PCXMC:ssä ei käsitellä muita vuorovaikutustyyppejä, koska maksimifotonienergia on laskennassa rajattu arvoon 150 keV. Kussakin vuorovaikutuksessa tallennetaan luovutettu energia sille elimelle, missä vuorovaikutus tapahtuu. Kunkin fotonin vuorovaikutustapahtumat muodostavat ns. yksittäisen fotonin historian. Laskennassa generoidaan suuri määrä yksittäisten fotonien historioita, joista arvioidaan eri elimiin absorboituneiden energioiden odotusarvot, joista saadaan elinten annokset.

Laskettuja elinten annoksia voidaan käyttää arvioimaan säteilystä aiheutuvaa syöpäkuoleman riskiä. Riskiarviot perustuvat BEIR VII -komitean (BEIR 2006) kehittämien suhteellisen ja absoluuttisen riskimallin yhdistelmään. PCXMC arvioi säteilyn aiheuttaman kuoleman riskin leukemialle, paksusuolen syövälle, mahasyövälle, keuhkosyövälle, virtsarakon syövälle, eturauhasen syövälle, kohtusyövälle, munasarjasyövälle, rintasyövälle, maksasyövälle ja kilpirauhassyövälle sekä tekee yhteisarvion muille syöville. Ohjelman käyttäjä voi käyttää riskinlaskentaosiota arvioon, jossa tarkastellaan joko yhden kuvan tai useasta kuvasta koostuvan röntgentutkimuksen aiheuttamaa riskiä, kun elinten annokset on arvioitu PCXMC:n avulla. Ohjelman käyttäjä voi myös asettaa elinannokset haluamikseen, laskematta niitä PCXMC:n avulla: riskilaskenta voidaan tehdä mielivaltaiselle säteilyaltistustilanteelle.

Ohjelman nykyinen versio (2.0) toimii PC-tietokoneessa, jossa on käyttöjärjestelmänä Windows 95, 98, NT, 2000, XP tai Vista. Monte Carlo -laskentaan kuluva aika riippuu laskennassa halutusta tarkkuudesta ja PC:n nopeudesta, mutta on tyypillisesti alle minuutin, kun käytetään PC:tä, jonka kellotaajuus on 1.8 GHz. Samaa Monte Carlo -laskennasta saatua dataa voidaan käyttää laskettaessa toisen röntgensäteilyspektrin tai säteilymäärän aiheuttamia annoksia, kunhan muut röntgentutkimukseen liittyvät tekijät pysyvät samoina. Tällaisten erilaisten altistusten laskenta-ajat ovat erittäin pienet, koska niiden laskentaan ei tarvita uutta Monte Carlo -simulointia.

PCXMC:n avulla laskettuja tuloksia on jo aiemmin verrattu Jonesin ja Wallin (1985) ja Hartin ym. (1994, 1996) NRPB:ssä laskemiin annosmuuntokertoimiin,

ja niiden on todettu vastaavan toisiaan hyvin (Tapiovaara ym. 1997). Tämä hyvä yhteensopivuus NRPB:n datan kanssa on edelleen voimassa valtaosalle röntgenkuvaustilanteita. Joissakin tilanteissa havaitaan nyt kuitenkin pienehköjä eroja, koska laskennassa käytettyjen fantomien muotoa, kudosten koostumusta ja tiheyttä on muutettu ohjelman aikaisemmista versioista. PCXMC:n tulokset ovat vastanneet kohtuullisen hyvin myös monien muiden mittausten ja laskentamallien tuloksia, esim. Schmidt ym. (2000), Schultz ym. (2003), Helmrot ym. (2007). PCXMC:n fantomien kokomuunnoksen käyttökelpoisuus myös ääritilanteessa on todettu Smansin ym. (2008) julkaisemassa artikkelissa, jossa laskettiin kahden erikokoisen keskoslapsen (590 g ja 1910 g) annoksia. Heidän vokselifantomeillaan laskettujen annosten erot PCXMC:llä laskettuihin annoksiin selittyivät fantomimallien eroilla ja vaikeudella kohdistaa samanlainen säteilykeila erilaisiin fantomeihin niin, että altistustilanteet olisivat tarkasti vertailukelpoiset. Samansuuruisia eroja nähdään yleisesti, kun verrataan matemaattisten fantomien ja vokselifantomien avulla laskettuja annoksia (Staton ym. 2003, Lee ym. 2006 ja Pazik ym. 2007); samansuuruisia eroja saadaan myös, kun verrataan annoslaskuja, joissa on käytetty erilaisia vokselifantomeita (Zankl ym. 2002, Schlattl ym. 2007). Riskiarviotulokset ovat sopusoinnussa BEIR VII -komitean (BEIR 2006) raportissa annettujen arvojen kanssa.

Contents

1 Introduction

X-ray diagnostics is a significant source of radiation exposure among the population. Therefore, it is important that x-ray examinations are conducted using techniques that keep the patients' exposure as low as possible but still compatible with the medical purposes of the examinations (ICRP 1996). In order to achieve this, it is necessary to understand the factors that affect the exposure and to be able to assess the patients' doses.

Patient dose is often described by the patient's entrance surface dose, which is measured on the patient's skin at the centre of the x-ray beam. An alternative to this is to make the measurement free-in-air, without the contribution of the radiation that is backscattered from the patient, and express the result in terms of air kerma (incident air kerma, ICRU 2005). In some cases such simple measurements may be sufficient. This is the case, for example, in quality control measurements which concern the stability of equipment, and where the same x-ray exposure conditions are used in each measurement. However, the entrance surface dose is not sufficient for comparison or assessment of patients' doses if the irradiation conditions (the size of the patient, the radiation quality, the exposed body-part, or other factors) are changed. In such cases, the patient dose needs to be characterised by quantities that are more directly related to the detriment caused by radiation (ICRU 2005). Optimisation of imaging techniques is an example of a case where the incident air kerma or the entrance surface dose are not sufficient for quantifying the patient dose, unless the local skin dose –not cancer induction– is the primary concern.

Presently, stochastic harm to humans from ionising radiation is assessed by the mean absorbed doses (or equivalent doses) in various organs or tissues in the body (ICRP 2007). For some purposes, the detriment can be assessed – and reported more simply– by referring to the effective dose: this enables one to express the dose as a single number, instead of a list of doses in various organs and tissues. However, the use of the effective dose in describing the radiation exposure of patients is sometimes criticized and it is suggested that appropriate risk values for the individual tissues at risk should be used instead (ICRP 2007). Therefore, also the ability of assessing the risk of exposure-induced cancer has been built to PCXMC 2.0. The risk assessment is done according to the model of BEIR VII Committee (BEIR 2006).

Organ doses and the effective dose cannot be measured directly in patients undergoing x-ray examinations, and they are difficult and time consuming to obtain by experimental measurements using physical phantoms. However, they can be calculated to a reasonable approximation, provided that sufficient data on the x-ray examination technique are available. Today, such calculations are

most often made using the Monte Carlo calculation method, where random numbers are used for simulating the transport of radiation in a complex medium, in this case the human body. [For references on the Monte Carlo method in medical applications, see, for example, Andreo (1991).] The physical interactions between radiation and matter are sufficiently well-known, and the accuracy of the calculation is limited mainly by the accuracy of the anatomical model used to describe actual patients and by the characterisation of the applied radiation field (Zankl et al. 1989, Jones and Wall 1985).

Monte Carlo data on organ doses and the effective dose in general projection radiography of adults have been presented in tabular form in Rosenstein (1976a and 1976b), Rosenstein et al. (1992), Jones and Wall (1985), Drexler et al. (1990), Hart et al. (1994a and 1994b) and Stern et al. (1995). Similar data for children have been presented in Rosenstein et al. (1979), Zankl et al. (1989) and Hart et al. (1996a and 1996b). Such data and the methods for obtaining them have been reviewed in ICRU Report 74 (2005). Recently, Kramer et al (2008) have published a computer program which contains, among other data, conversion coefficients for 34 x-ray projections and 40 x-ray spectra; their conversion coefficients have been calculated using voxel-based adult male and female phantoms. In addition to these tabulated conversion factors, several publications consider special cases of x-ray examinations and give dose conversion factors for them. In spite of the extensive tabulation of organ dose conversion factors in the above-mentioned references, not all x-ray projections or x-ray spectra of interest are covered and the data apply only for those individuals whose size and body-build correspond to the phantoms used in deriving the data.

Radiation and Nuclear Safety Authority, Finland (STUK) first published PCXMC (PC program for X-ray Monte Carlo) in 1997 (Tapiovaara et al. 1997). This program allowed computation of organ doses for patients of different ages and sizes in freely adjustable x-ray projections and other examination conditions that are used in projection radiography and fluoroscopy. Since 1997, the program has been improved in several occasions. PCXMC versions 1.0–1.5 used slightly modified mathematical phantom models of Cristy (1980). In the present version (PCXMC 2.0) the phantom is still basically the same, but has been updated to the phantom models of Cristy and Eckerman (1987) with some further modifications (modification of the head, correction of some apparent errors in the data of Cristy and Eckerman and inclusion of some new organs: extrathoracic airways, oral mucosa, prostate and salivary glands). These modifications of the phantom enable the calculation of the effective dose using the tissue weighting factors introduced in ICRP Publication 103 (2007). The program is now also able to assess age- and sex-dependent radiation risks.

The Monte Carlo simulation time depends on the desired accuracy and on the speed of the PC, but takes typically from a few seconds to a few minutes with a PC with a 1.8 GHz processor. After having made the Monte Carlo calculation once, the user can calculate the organ doses for various x-ray spectra with a minimal computation time.

2 Radiation dose quantities in PCXMC

All organ doses calculated with PCXMC are given in proportion to the incident air kerma ($K_{a,i}$) which is measured free-in-air, without backscatter, at the point where the central axis of the x-ray beam enters the patient. The incident air kerma – or, alternatively, the exposure (X; in mR), the air kerma-area product (P_{KA}, KAP or DAP; in mGy·cm^2) or the exposure-area product (in R·cm^2) – must be supplied by the user of the program. This datum can be calculated from the technique factors [x-ray tube voltage (kV), tube current-time product (mAs), total filtration and focal spot-to-skin distance (FSD)] and measured data of the radiation output of the x-ray source, or it can be obtained from entrance surface air kerma measurements or DAP measurements of actual patient examinations. If no actual radiation measurements are available, one can use the ability of PCXMC to estimate $K_{a,i}$ with a reasonable accuracy from the x-ray tube current-time product (mAs); the other necessary parameters [the x-ray tube voltage (kV), the total filtration in the radiation beam and the distance from the x-ray tube focal spot to the patient's skin (FSD)] must anyway be input by the user.

If the entrance surface air kerma ($K_{a,e}$) or the entrance surface dose (ESD) at the centre of the x-ray beam has been measured on the patient's skin and includes radiation back-scattered from the patient, the dose must be divided by the backscatter factor (BSF) before using it in PCXMC. The BSF depends on the x-ray spectrum and beam size and is typically of the order of 1.3–1.4. The practical range of BSF is 1.1–1.6. For data on the BSF, see, for example, Grosswendt (1990), Petoussi-Henss et al. (1998) or ICRU (2005); some typical BSF values (Petoussi-Henss et al. 1998) are shown in Table I.

Table I. Backscatter factors (BSF) for three field sizes and some x-ray spectra typical in diagnostic radiology. (FSD 100 cm, ICRU phantom tissue.) (Petoussi-Henss et al. 1998).

X-ray tube voltage (kV)	Filtration	HVL (mm Al)	BSF		
			10×10 cm²	20×20 cm²	25×25 cm²
50	2.5 mm Al	1.74	1.25	1.27	1.28
60	2.5 mm Al	2.08	1.28	1.32	1.32
70	2.5 mm Al	2.41	1.31	1.36	1.36
70	3.0 mm A+0.1 mm Cu	3.96	1.39	1.47	1.47
80	2.5 mm Al	2.78	1.33	1.39	1.39
80	3.0 mm A+0.1 mm Cu	4.55	1.40	1.50	1.51
90	2.5 mm Al	3.17	1.34	1.41	1.42
90	3.0 mm A+0.1 mm Cu	5.12	1.41	1.51	1.53
100	2.5 mm Al	3.24	1.34	1.41	1.42
100	3.0 mm A+0.1 mm Cu	5.65	1.42	1.53	1.55
110	2.5 mm Al	3.59	1.35	1.43	1.44
120	3.0 mm A+0.1 mm Cu	6.62	1.42	1.54	1.56
130	2.5 mm Al	4.32	1.36	1.45	1.47
150	2.5 mm Al	4.79	1.36	1.46	1.48
150	3.0 mm A+0.1 mm Cu	8.50	1.41	1.54	1.57

If the patient's entrance dose has been measured in terms of tissue dose instead of air kerma, the measured datum must be converted to air kerma before using it as an input to the program. Strictly, the conversion from tissue dose, D_{tissue}, to air kerma, K_a, depends on the composition of the tissue and the energy spectrum of radiation. For the energies of diagnostic radiology, the approximate relationship $K_a = 0.94 \cdot D_{soft\ tissue}$ can be used. In the photon energy range considered in PCXMC (photon energies less than 150 keV), kerma in tissue and absorbed dose in tissue can be considered equivalent (except in bone-soft tissue interfaces, see chapter 4 below).

PCXMC calculates the mean values of absorbed doses, averaged over the organ volume, for the organs shown in Table II[1]. In addition to these organ doses, the program calculates the effective dose for both the present tissue weighting factors w_T (ICRP 2007) and the old ones (ICRP 1991)[2]. PCXMC also calculates the average absorbed dose in the whole body, and the fraction of the x-ray beam energy that is absorbed in the phantom. In PCXMC, all absorbed doses (and air kerma) are in milligray (mGy). For photons, the numerical values of the

[1] In order to avoid ambiguity, it is noted that in PCXMC 'skin dose' refers to the mean value of absorbed dose averaged over the whole skin of the phantom.

[2] For later modifications of this 'old effective dose' as used in PCXMC see, e.g., ICRP (1995)

equivalent doses of organs in millisieverts (mSv) are equal to the corresponding organ doses in mGy. The unit of the effective dose is mSv.

In PCXMC the calculation of effective dose is not strictly done according to the specifications in ICRP Publication 103 (2007): in PCXMC, the effective dose is calculated using size-adjustable hermaphrodite phantoms, whereas the present ICRP (2007) definition specifies that the organ doses are calculated in a reference male phantom and in a reference female phantom, the equivalent organ doses in these two phantoms are averaged, and the effective dose is obtained as a weighted sum of these sex-averaged organ doses. This prescription cannot be easily followed in partial body exposures, such as x-ray imaging, where the field size and the quality and amount of radiation are adjusted according to the patient's size: an x-ray beam of specified size cannot be unambiguously directed similarly to two phantoms of different size and shape. This difficulty is avoided by using hermaphrodite phantoms.

The effective dose has been introduced to express a radiation detriment-related dose for radiation protection purposes in situations where the dose to the body is not uniform and the absorbed doses are low enough for avoiding deterministic radiation effects. The effective dose is given as a weighted average of the equivalent doses in various organs and tissues. In deriving the tissue weighting factors, an equal number of males and females and a wide range of ages in the exposed population were assumed. Therefore, and because of the health status difference of patients and general population, it may not always be reasonable to use this quantity in reporting doses from medical radiology; for critical views on the use of the effective dose in diagnostic radiology see Drexler et al. (1993) and Martin (2007). If the patient material considered differs greatly from the average population, the use of a different set of weighting factors and risk coefficients should be more appropriate (BEIR 1990, Stokell et al. 1993, Almén and Mattsson 1996). Such age- and sex-dependent weighting factors have not been agreed on; therefore, for example the ICRP uses the same set of tissue weighting factors for all ages and even for the developing foetus, although with caution (ICRP 2007).

The ICRP specifically stresses that effective dose should not be used for, e.g., the assessment of individual risk, assessment of the probability of causation of cancer, or for epidemiological studies. Absorbed doses to irradiated tissues should be used for these purposes. However, the ICRP acknowledges that the effective dose can be of value for comparing doses from different diagnostic procedures and for comparing the use of similar technologies and procedures in different hospitals and countries as well as the use of different technologies for the same medical examination (ICRP 2007). Effective dose has widely been used

for such purposes: for example in assessing the population dose from diagnostic x-ray examinations (e.g., UNSCEAR 2000, Hart and Wall 2002 and Scanff et al. 2008).

It should also be kept in mind that in partial body exposures local absorbed doses may be large even if the mean doses in organs or the effective dose are small. Therefore, low organ doses or a low effective dose do not necessarily imply avoiding deterministic radiation effects (tissue reactions) (ICRP 2007).

PCXMC calculates the effective dose for allowing easy comparisons e.g. between different diagnostic procedures. If a more detailed risk assessment is needed, the risk calculation capability of PCXMC should be used. This risk model is based on the report of BEIR VII committee (BEIR 2006), and takes into account, e.g., the sex, age at exposure and attained age of the patient (see chapter 6 for more details). Still, it has to be remembered that individual risk estimates are highly uncertain because of inherent uncertainties in the risk models, the health status of the individual in question and, e.g. individual sensitivity to radiation-induced cancer.

Table II. The organs considered in PCXMC, and their tissue weighting factors for the calculation of the effective dose according to both the present and the old ICRP definitions.

Organ or tissue	Tissue weighting factor w_T (ICRP 103) [7]	Tissue weighting factor w_T (ICRP 60) [8]
Active bone marrow	0.12	0.12
Breasts	0.12	0.05
Colon[1]	0.12	0.12
Lungs	0.12	0.12
Stomach	0.12	0.12
Ovaries (female gonads)[2]	0.08/2	0.20/2
Testicles (male gonads)[2]	0.08/2	0.20/2
Liver	0.04	0.05
Oesophagus	0.04	0.05
Thyroid	0.04	0.05
Urinary bladder	0.04	0.05
Brain	0.01	r
Bone surface[3]	0.01	0.01
Salivary glands	0.01	-
Skin	0.01	0.01
Adrenals	0.12/13	r
Extrathoracic airways[4]	0.12/13	r
Gall bladder	0.12/13	-
Heart	0.12/13	-
Kidneys	0.12/13	r
Lymphatic nodes[5]	0.12/13	-
Muscle[6]	0.12/13	r
Oral mucosa	0.12/13	-
Pancreas	0.12/13	r
Prostate (male)	0.12/26	-
Small intestine	0.12/13	r
Spleen	0.12/13	r
Thymus	0.12/13	r
Uterus (female)	0.12/26	r

1) The dose in the colon is calculated as the mass-weighted average of the upper large intestine and the lower large intestine.
2) The dose in the gonads is defined as the average of the doses in the ovaries and testicles. The tissue weighting factor for gonads is presently 0.08 (ICRP Publication 103) and was earlier 0.20 (ICRP Publication 60).
3) The tissue weighting factor refers to the dose to bone surface. PCXMC approximates this dose using the dose to the whole skeleton (excluding active bone marrow).
4) In PCXMC only the trachea, pharynx and nasal sinuses are used to represent the extrathoracic airways.
5) In PCXMC the lymph nodes have not been modelled in the phantom. The dose in lymph nodes is calculated as a weighted average of several surrogate organs (see chapter 3).
6) In PCXMC, the dose in muscle tissue is calculated as the average dose to the whole phantom, but excluding the other organs and tissues given in this table.
7) The weighting factors that are shown as the fraction 0.12/13 or 0.12/26 represent the remainder organs of ICRP 103. The new weighting factor for the arithmetic average of the remainder organs is given the tissue weighting factor 0.12. Sex-specific organs have effectively a lower weighting factor than the other remainder organs.
8) Weighting factors labelled as "–" denote organs that are not included in the calculation of the effective dose according to the old ICRP 60 definition. Weighting factors labelled as "r" belong to the 'remainder tissues' of ICRP Publication 60. The tissue weighting factor of the ICRP 60 remainder is 0.05, and is applied to the mass averaged dose in the remainder organs and tissues. However, if any of these organs receives a dose that is higher than the dose to any of the twelve organs for which a weighting factor is specified, a weighting factor of 0.025 is applied to that tissue or organ and the rest of the weighting factor, 0.025, is applied to the mass averaged dose in the other remainder organs and tissues (ICRP 1991 and 1995).

2.1 Incident air kerma calculation based on the tube current-time product (mAs)

PCXMC can evaluate the incident air kerma from the specified examination factors, when only the tube current-time product (mAs) is known. All other data needed for the evaluation: x-ray tube voltage (kV), total filtration and FSD, must be specified in the examination's input data anyway. This option cannot be used, if the user has specified the FSD to be infinite (actually: 100 m).

In practice, the x-ray tube output varies from one unit to the next, however, and one cannot expect an exact agreement between the calculated and measured incident air kerma. Variability between x-ray tubes is caused at least by differences in the following factors:

- x-ray tube voltage waveform (PCXMC assumes a constant potential or low-ripple generator)
- x-ray tube anode angle (not used in the incident air kerma calculation in PCXMC)
- smoothness of the x-ray tube anode surface
- actual filter materials in the beam path; [in spite of matching filtration equivalence, the attenuation of the actual filter (including glass and oil) may differ from the attenuation of an aluminium filter]
- differences in off-focal radiation and its removal by collimation
- the error between actual and displayed values of the tube voltage (kV), the tube current-time product (mAs) and the filtration.

The x-ray tube output calculation of PCXMC is based on x-ray tube output measurements from diagnostic x-ray tubes. The basic data have been obtained from 46 different x-ray tubes and/or filter choices. The average of these measurements agrees with the value calculated with PCXMC, and the standard deviation between the individual measured results and the calculated results is 16%. Therefore, one can expect the calculated output dose to be within about 30% (2 standard errors) of the correct value.

The ratio of calculated and measured results is typically constant for a given x-ray tube; the ratio typically stays the same although x-ray tube voltage or filtration is varied. This can be used to improve the accuracy of mAs-based dose calculations. By making x-ray tube output measurements for a given x-ray system and comparing these with the output values calculated by PCXMC one will get an effective 'mAs calibration coefficient' for that x-ray tube, and it can be used at all x-ray tube voltages and filter choices. By doing such a normalisation for each of the 46 x-ray tubes above, the standard deviation between individual measured and calculated results dropped to 5%, and the accuracy of the calculation can then be taken as 10%.

3 Mathematical phantoms

Several phantom models are available for representing the human body in Monte Carlo calculations (e.g., Kramer et al. 1982, Cristy and Eckerman 1987, ICRU 1992a, Lee et al. 2006a, Schlattl et al. 2007). These include voxel-phantoms, which are based on CT and MR images of actual human beings, and computational models where body contours and organs are defined by mathematical expressions.

The phantoms used in PCXMC version 2.0 are computational hermaphrodite phantoms representing human beings of various ages (new-born, 1, 5, 10, 15-year-old and adult). These phantoms have been specified by Cristy and Eckerman (1987), but a few modifications, explained below, have been made in PCXMC. The principal body dimensions of these phantoms are given in Table III, and the composition of their tissues is shown in Table IV. The phantom models used in earlier versions of PCXMC were somewhat different: they were modelled according to Cristy (1980) with small modifications (Tapiovaara et al. 1997).

Table III. Principal dimensions of the mathematical phantoms as modified in PCXMC 2.0. In the calculation the user can specify whether the arms of the phantom are included at the sides of the trunk or whether they are removed (which may simulate the real situation better, e.g., for lateral projections). Trunk width is given for both of these conditions. Phantom height and weight have changed from the earlier PCXMC versions.

	Weight (kg)	Total height (cm)	Trunk height (cm)	Trunk thickness (cm)	Trunk width[1] (cm)	Trunk width[2] (cm)	Leg length (cm)
Newborn	3.40	50.9	21.6	9.8	10.94	12.7	16.8
1 year old	9.20	74.4	30.7	13.0	15.12	17.6	26.5
5 year old	19.0	109.1	40.8	15.0	19.64	22.9	48.0
10 year old	32.4	139.8	50.8	16.8	23.84	27.8	66.0
15 year old	56.3	168.1	63.1	19.6	29.66	34.5	78.0
Adult	73.2	178.6	70.0	20.0	34.40	40.0	80.0

[1] excluding arms

[2] including arms

Table IV. Elemental composition of the phantom tissues as used in PCXMC 2.0 (% by weight). The number of elements has been reduced from that in Cristy and Eckerman (1987) by grouping the elements Na, Mg, P, S, and Cl together and treating them as phosphorus, and grouping all elements of atomic numbers from that of K or higher together and treating them as calcium. The density and composition have changed from the earlier PCXMC versions.

	Density (g/cm^3)	H (%)	C (%)	N (%)	O (%)	P (%)	Ca (%)
Skeleton (except newborn)	1.40	7.337	25.475	3.057	47.893	5.876	10.362
Newborn skeleton	1.22	7.995	9.708	2.712	66.811	4.623	8.151
Lung tissue	0.296	10.134	10.238	2.866	75.752	0.770	0.240
Other soft tissues (except newborn)	1.04	10.454	22.663	2.490	63.525	0.626	0.242
Other soft tissues (newborn)	1.04	10.625	14.964	1.681	71.830	0.592	0.308

The phantom models of Cristy and Eckerman (1987) were intended to be used for dosimetry of internal photon sources. After their publication, the head and neck region and the upper part of the spine of the phantoms have been modified by Eckerman and Ryman (1993) in order to have the phantom models better suited for external irradiation calculations. These modifications are explained in more detail in Eckerman, Cristy and Ryman (1996). Eckerman and Ryman (1993) also added the oesophagus among the organs in the phantoms. These modifications have also been included in PCXMC 2.0, although with small further modifications:

- The back of the head has been modelled as a circular cone, rather than as an elliptic cylinder as in Eckerman, Cristy and Ryman (1996). For an example of the old and new head and neck area, see Figure 1. The head model of PCXMC resembles, but is not equal to, the MIRD head model (Bouchet et al. 1999).
- The lateral width of the facial skeleton has been reduced from the value given in Cristy and Eckerman (1987) in order to make room for the parotid glands.
- The apparent error in the vertical location of the facial skeleton in the data of Eckerman, Cristy and Ryman (1996) has been corrected, and the facial skeleton is located in a lower position than where it would be according to their data.
- The apparent error in the position of the thyroid in the data of Eckerman, Cristy and Ryman (1996) has been corrected. The data used in PCXMC for the adult phantom corresponds to the data given in Eckerman and Ryman (1993).
- Salivary glands (parotid, sublingual and submandibular glands) have been modelled in the phantoms. The size and location of the glands were derived from data in ICRP Publication 89 (ICRP 2002) and Möller and Reif (1994a).
- Extrathoracic airways (pharynx, larynx, part of trachea, paranasal sinuses) have been modelled in the phantoms. Guidance for the modelling was obtained from Möller and Reif (1994a). Mouth has not been considered as a part of extrathoracic airways, although it is among the extrathoracic airway tissues mentioned in ICRP Publication 89 (ICRP 2002). Mouth mucosa is treated separately in PCXMC.
- Mouth mucosa has been modelled in the phantoms. Part of the tissue is located between the skin and the facial skeleton, and another part behind the facial skeleton.
- The prostate has been modelled in the phantoms. Guidance for the modelling was obtained from ICRP Publication 89 (ICRP 2002) and Möller and Reif (1994b).

- The arms of the phantoms can be removed in order to enable more realistic calculations for lateral x-ray projections. When the user chooses this option, it is realised by cutting the trunk region with two planes, which are parallel to the y-z plane, and located at the maximum dimension of the rib cage in the direction of the x-axis, but increased by the thickness of the skin. (The origin of the coordinate system is located at the middle of the base of the trunk of each phantom; the z-axis points upwards, the x-axis to the left-hand side of the phantom, and the phantom looks in the negative y-direction.)
- The height and mass of the phantoms can be varied and matched to the data of individual patients. This feature is explained in more detail below.
- Lymph nodes have not been modelled in the phantoms. Instead, the dose in the lymph nodes is estimated from the doses in surrogate organs as

$$\begin{aligned} D_{\text{lymph nodes}} = {} & 0.25 \cdot D_{\text{small intestines}} + 0.15 \cdot D_{\text{pancreas}} + \\ & 0.13 \cdot D_{\text{extrathoracic airways}} + 0.10 \cdot D_{\text{gall bladder}} + \\ & 0.08 \cdot D_{\text{salivary glands}} + 0.07 \cdot D_{\text{lungs}} + \\ & 0.05 \cdot D_{\text{thyroid}} + 0.05 \cdot D_{\text{total body}} + \\ & 0.04 \cdot D_{\text{oesophagus}} + 0.04 \cdot D_{\text{heart}} + \\ & 0.03 \cdot D_{\text{stomach}} + 0.01 \cdot D_{\text{testes}} . \end{aligned} \quad (1)$$

These surrogate organs and the weights in the averaging have been chosen with the guidance of the data given in Qatarneh et al. (2006), Möller and Reif (1994a and 1994b) and ICRP Publication 89 (ICRP 2002).

(a) (b)

Figure 1. An example of the head and neck area of the adult phantom, displayed with the "radiograph"-image in (a) PCXMC 2.0 (new model), (b) PCXMC 1.5 (modelled according to Cristy 1980). The head and neck model in the new version (2.0) is notably more appropriate for external irradiation dose calculations. The model of Eckerman, Cristy and Ryman (1993) would be in between these two models and would have excess soft tissue material at the back of the head: their head model is an elliptical cylinder topped by half an ellipsoid. The skeleton is shown in white, the thyroid in pink, the airways in blue, and the oesophagus in yellow colour. (Colours are seen only in the electronic document version.)

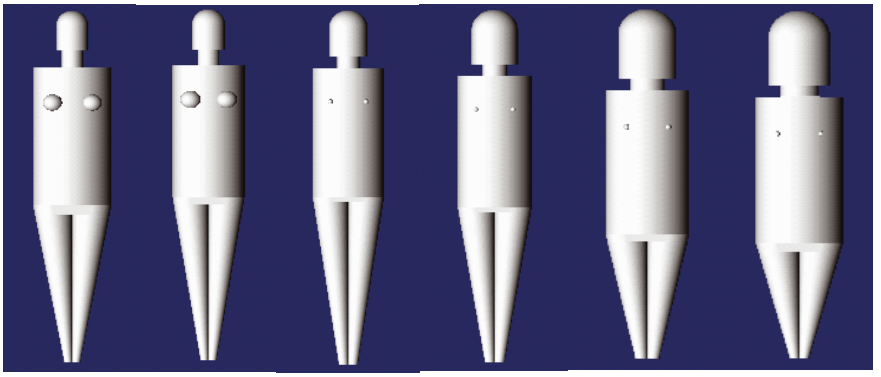

(a) (b) (c) (d) (e) (f)

Figure 2. Anterior views of the basic phantom models in PCXMC, scaled to have identical heights. (a) Adult phantom 178.6 cm/73.2 kg, (b) 15-year old phantom 168.1 cm/56.3 kg, (c) 10-year old phantom 139.8 cm/32.4 kg, (d) 5-year old phantom 109.1 cm/19.0 kg, (e) 1-year old phantom 74.4 cm/9.2 kg (f) new-born phantom 50.9 cm/3.4 kg.

Figure 2 illustrates the exterior shapes of the basic phantom models. PCXMC allows further modification of these basic phantoms by letting the user change the mass (M) or height (h) of any of them. Using these target body size values, the program calculates the scaling factors

$$s_z = \frac{h}{h_0} \tag{2}$$

and

$$s_{xy} = \sqrt{\frac{h_0 \cdot M}{h \cdot M_0}}\ , \tag{3}$$

where s_z is the scaling factor in the direction of the z-axis (phantom height), s_{xy} the scaling factor in the directions of the x- and y-axes (phantom width and thickness, respectively), and h_0 and M_0 are the height and weight of the unscaled phantom (Table III). All dimensions of the phantoms are then multiplied by these scaling factors, and the organ masses are changed accordingly. The coordinates corresponding to the transformed phantom, (x, y, z), are obtained from the coordinates of the same anatomical point corresponding to the basic phantom, (x_o, y_o, z_o), by

$$\begin{aligned} x &= s_{xy}\, x_o \\ y &= s_{xy}\, y_o \\ z &= s_z\, z_o. \end{aligned} \tag{4}$$

This operation allows the shape of the phantoms to be modified to resemble that of the actual patient more closely. It should be noted, however, that all measures in a given direction (i.e., vertical or horizontal) are being multiplied by the same scaling factor, and phantom shape variability due to, e.g., variability in the amount of fat tissue cannot be simulated by this method. An example of the height and weight transformation of the phantom is shown in Figure 3. This transformation does not have any effect on the coordinate system used for entering the x-ray beam geometry: the origin remains at the centre of the base of the trunk. The location of the organs will change, and the input coordinates of the x-ray beam have to be changed accordingly in order to simulate the irradiation of the same body part.

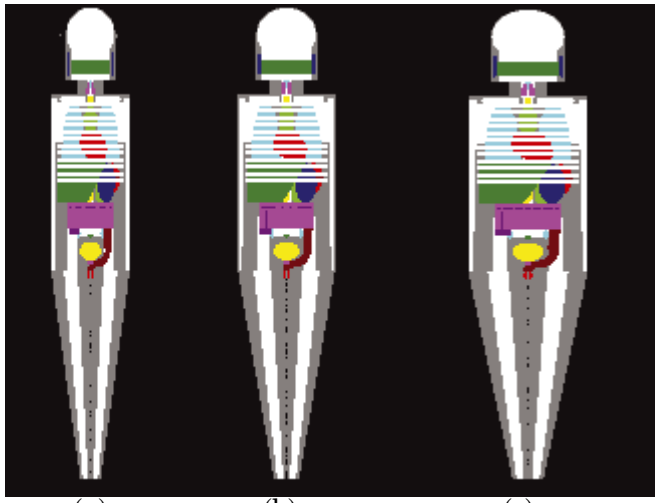

Figure 3. An example of the effect of the patient size transformation. The phantoms shown represent 5-year-old patients of height 109.1 cm with various mass: (a) 12.45 kg, (b) 19.0 kg, (c) 29.0 kg. The figure shows the body outline and the location of internal organs and the skeleton as seen from the front of the phantom.

4 The Monte Carlo method

Monte Carlo calculation of photon transport is based on stochastic mathematical simulation of the interactions between photons and matter (for a review and general references on Monte Carlo techniques see, e.g., Andreo 1991). Photons are emitted (in a fictitious mathematical sense) from an isotropic point source into the solid angle specified by the focal distance and the x-ray field dimensions, and followed while they randomly interact with the phantom according to the probability distributions of the physical processes that they may undergo: photo-electric absorption, coherent (Rayleigh) scattering or incoherent (Compton) scattering. This chain of interactions forms a so-called photon history. The cross sections for the photo-electric interaction, coherent scattering and incoherent scattering have been taken from Storm and Israel (1970) and the atomic form factors and incoherent scattering functions from Hubbell et al. (1975). Other interactions are not considered in PCXMC, because the maximum photon energy is limited to 150 keV. At these energies the range of secondary electrons in soft tissue is only a fraction of a millimetre, and the energy of the secondary electrons is approximated to be absorbed at the site of the photon interaction (except in calculating the bone marrow dose, see below). At each interaction point the energy deposition to the organ at that position is calculated and stored for dose calculation. A large number of independent random photon histories is generated, and estimates of the mean values of the energy depositions in the various organs of the phantom are used for calculating the dose in these organs.

Pseudo random numbers are generated by a multiplicative linear congruential generator, MLCG(16807, 2^{31}-1) (Vattulainen et al. 1993), and are used for sampling the initial photon direction, distance between interactions, type of interacting atom, type of interaction and scattering angle (and the corresponding energy loss). To improve the precision, the photons are constrained not to be absorbed by the photo-electric interaction; instead, the photo-electric absorption has been treated by associating a 'weight' to the photons. This weight, w, represents the expected proportion of photons that would have survived absorption in the preceding interactions, and is reduced in each interaction according to the probability of photo-electric absorption (p). At each interaction, an energy deposition of $w \cdot p \cdot E + w \cdot (1-p) \cdot \Delta E$ is made to the organ where the interaction occurs, and the photon weight is reduced to $w_{new} = w_{old} \cdot (1-p)$. Here, E is the photon energy before the interaction and ΔE the energy loss in the scattering interaction. Each photon is followed until it exits the phantom without hitting it again, its energy falls to less than 2 keV (in which case it is forced to be absorbed), or until its weight is reduced to less than 0.003. In the last case, the photon is subjected to a game of Russian roulette: it is discarded with a

probability of 0.75, but if it survives its weight is multiplied by a factor of four. Characteristic radiation resulting from the excitation of atoms in the body is not simulated, but it is assumed to be absorbed at the primary interaction site. There are no heavy elements in the phantoms; the maximum energy of such characteristic quanta would be about 4 keV and they would be absorbed near the primary interaction site.

The bones of the mathematical phantoms are modelled as a homogeneous mixture of mineral bone and organic constituents of the skeleton, including active bone marrow. The overall composition of the skeleton is approximated as being constant over all bones in the body (see Table IV), but the amount of active bone marrow is varied from one part of the skeleton to another and is different for phantoms representing different ages (Cristy and Eckerman 1987). In reality, active bone marrow is located in small cavities in trabecular bone which causes the dose in the bone marrow to be higher than the kerma, due to secondary electrons from the bone matrix. This must be taken into account when calculating the dose to the active bone marrow. PCXMC calculates the dose in both components of the skeleton, the active bone marrow and the rest of skeletal material, by dividing the absorbed energy in the whole skeleton into two parts: active bone marrow and other constituents of bone (e.g., Rosenstein 1976a). For an energy deposition ΔE in a specific skeletal part i from a photon with energy E, the part of energy deposited in the active bone marrow in that skeleton part, $\Delta E_{ABM,\,i}$, is calculated by

$$\Delta E_{ABM,\,i} = \Delta E \cdot \frac{\left(\mu_{en}(E)/\rho\right)_{ABM}}{\left(\mu_{en}(E)/\rho\right)_{bone}} \cdot \frac{m_{ABM,\,i}}{m_{bone,\,i}} \cdot f_i(E) \tag{5}$$

where $m_{bone,\,i}$ and $m_{ABM,\,i}$ denote the mass of the skeleton part i, and the mass of active bone marrow in that skeleton part, respectively. $\mu_{en}(E)/\rho$ is the mass-energy absorption coefficient. The influence of the small cavity size on the dose in the active bone marrow is considered by multiplication with a photon energy dependent kerma-to-dose conversion factor (or dose enhancement factor), $f_i(E)$, which increases the active bone marrow dose by a few percents when compared to the kerma (Kerr and Eckerman 1985, King and Spiers 1985). The size of the bone marrow cavities may vary depending on the age or the anatomical part of the skeleton (King and Spiers 1985), but this has not been taken into account in PCXMC: the same factor (Figure 4) is used for all bones and all phantom ages. The energy deposition in the other constituents of the skeleton (all other bone material than active bone marrow) is then $\Delta E - \Delta E_{ABM,\,i}$. The dose in the active bone marrow is calculated as a sum over all energy depositions and all parts of the skeleton according to Equation (5), divided by the total mass of active bone

marrow. For a discussion of various methods of calculating dose in the active bone marrow see the paper of Lee et al. (2006b).

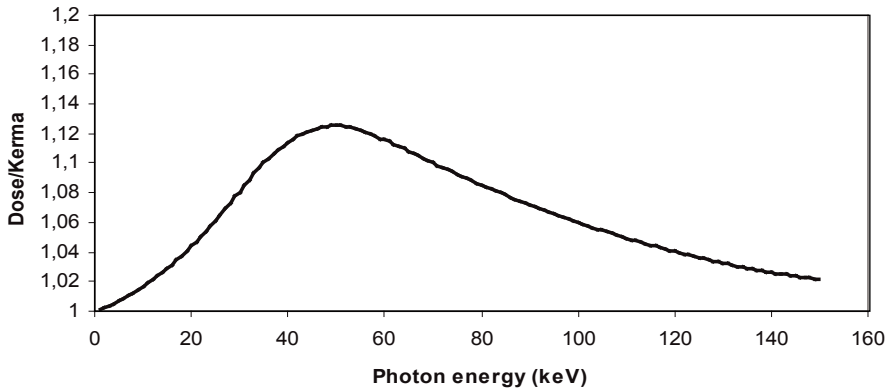

Figure 4. The kerma-to-dose conversion factor for active bone marrow in the lumbar vertebra (Kerr and Eckerman 1985). PCXMC uses this curve for all bone marrow sites.

PCXMC calculates the organ doses for monochromatic photons of 10, 20, ..., 150 keV energy [or up to an user-defined maximum (which is below 150 keV)] in ten different batches of each energy value. This is sufficient, because the absorbed energy per photon is a smooth function of photon energy in any organ; the value of absorbed energy per photon at other photon energies can be obtained with sufficient accuracy by linear interpolation. The final estimate of the absorption at each simulated energy value is obtained as the average of these batches, and the statistical error is estimated from the standard deviation of these batches. The doses and their statistical errors for a practical x-ray spectrum of interest are calculated afterwards by another module included in the program. The same Monte Carlo data can, therefore, be used for calculating doses for any spectrum of interest; such calculations are fast because they do not involve any further Monte Carlo simulations.

The x-ray spectra are calculated according to the theory of Birch and Marshal (1979) and are specified in terms of the x-ray tube voltage (kV), the angle of the tungsten target of the x-ray tube, and filtration. In the present version of the program, the user can simultaneously define two filters of arbitrary atomic number and thickness. The filter data are from the compiled x-ray interaction data of McMaster et al. (1969). Air kerma is calculated from photon fluence data using the conversion coefficients in ICRU (1992b) and Büermann et al. (2006).

It should be noted that the precision of both the dose estimate and the estimate of its statistical error depend on the number of simulated interactions in the organ. The precision may be poor even for a large number of simulated photon histories if the dose in the organ is low or the organ small. It should also be noted that when the number of interactions is small, which is indicated by a high value of the statistical error, the estimate has a skewed non-normal distribution and the actual statistical errors may be higher than expected on the basis of the standard deviation.

5 Comparison with other data

The data calculated with PCXMC versions 1.2–1.5 have been earlier compared to the organ dose conversion factors calculated in NRPB by Jones and Wall (1985) and Hart et al. (1994b, 1996b) and were found to agree well. This agreement was to be expected, because also their data were calculated using the phantom models of Cristy (1980). Reasonable agreement of PCXMC results has also been found in many comparisons with other dose calculations and phantom models or dose measurements, e.g., Tapiovaara et al. (1997), Schmidt et al. (2000), Schultz et al. (2003) and Helmrot et al. (2007). The agreement with the NRPB data still exists for PCXMC 2.0 for most irradiation conditions. Small differences are evident in some irradiation conditions, because the composition and density of the phantom tissues have been changed and the phantoms have been modified from the earlier versions of the program. This is depicted in Figure 5, which compares doses in some organs calculated with PCXMC versions 1.5.2 and 2.0 for a PA-direction photon irradiation of the head and neck. As can be expected from the differences in the phantom models, doses to the brain and thyroid are higher in the new version, whereas the dose in the muscle tissue is lower. The change in the oesophagus model and the change in the composition of active bone marrow also result in differences between these program versions.

Figures 6 and 7 compare organ dose data for two x-ray examinations, adult PA chest and paediatric AP abdomen, from PCXMC versions 1.2 and 2.0 and the data of NRPB. For the purpose of comparison, the NRPB data below have been renormalized to correspond to an air kerma (free-in-air) of 1 Gy. It is seen that in these examinations the conversion factors of most organs have not changed appreciably from the earlier versions of PCXMC. Exceptions to this are the active bone marrow, oesophagus and thyroid, where changes in the composition, modelling or surroundings, respectively, have been made. Similar changes can be expected also for other organs that have been modified from the earlier version, e.g. the breast of the 15-year-old phantom.

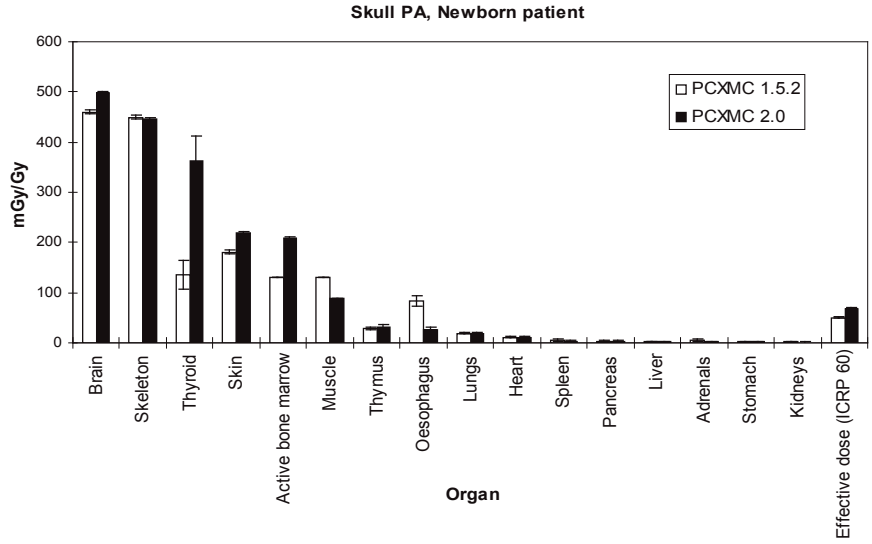

Figure 5. A comparison of the organ dose conversion factors calculated by PCXMC versions 1.5.2 and 2.0. All doses correspond to an entrance air kerma (free-in-air) of 1 Gy. Newborn patient, irradiation of the head and neck, PA projection, FSD 100 cm, x-ray tube voltage 70 kV, filtration 3 mm Al, 17° x-ray tube anode angle. The error bars shown correspond to two standard errors of the data.

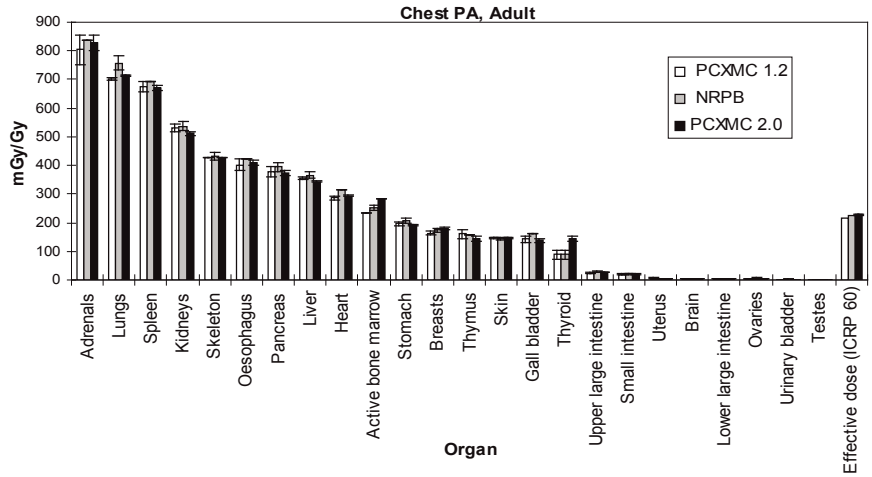

Figure 6. A comparison of the organ dose conversion factors calculated by PCXMC versions 1.2 and 2.0 with the data of Jones and Wall (1985 , NRPB data with error bars) and Hart et al. (1994b, NRPB data without error bars). All doses correspond to an incident air kerma of 1 Gy. Adult patient, chest examination, PA projection, x-ray tube voltage 120 kV, filtration 3 mm Al, 17° x-ray tube anode angle, FSD 160 cm. The error bars shown correspond to two standard errors of the data.

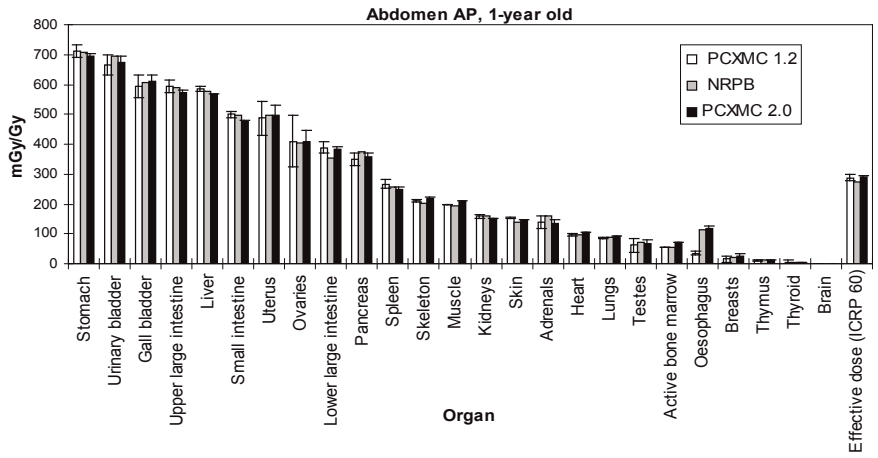

Figure 7. A comparison of the organ dose conversion factors calculated by PCXMC versions 1.2 and 2.0 with the data of Hart et al. (1996b). All doses correspond to an entrance air kerma (free-in-air) of 1 Gy. 1-year-old patient, abdomen examination, AP projection, x-ray tube voltage 70 kV, filtration 3 mm Al, 17° x-ray tube anode angle, FSD 92 cm. The error bars shown correspond to two standard errors of the data.

As was already noted above, the organ doses calculated are strictly valid only for the phantoms used for the calculation. To illustrate differences between different phantom models, we have compared organ dose conversion data calculated with PCXMC to the data of Schlattl et al. (2007) who have calculated dose conversion factors for whole body external exposure of photons using voxel phantoms 'Rex' and 'Regina' that are expected to be adopted as the standard human models by the ICRP. Figure 8 shows their conversion coefficient from air kerma to effective dose as a function of photon energy for total body irradiation from the front (AP-direction) and back (PA-direction). The conversion factors of PCXMC have been calculated as an average of the effective doses of two adult phantoms which have been matched to the height and mass of Rex and Regina. The agreement between the data calculated with PCXMC and the data of Schlattl et al. (2007) is remarkable in the AP irradiation case, and reasonable in the PA irradiation case.

Figure 9 shows the photon energy dependence of the conversion coefficient from air kerma to the dose in salivary glands. The data of Schlattl et al. (2007) are given for both their phantoms, Rex and Regina, and the data calculated with PCXMC are obtained by hermaphrodite phantoms matched to the height and mass of Rex and Regina.

The largest difference between the dose conversion factors of Schlattl et al. (2007) and PCXMC are in the doses in bones: the values calculated with PCXMC are about 50% larger, depending on the photon energy. This is probably

due to the difference in bone modelling. PCXMC uses the homogeneous bone-approximation whereas the bone model of Schlattl et al consider cortical bone and spongiosa separately and calculate the dose in the spongiosa only: the effect of the cortical part is to shield the spongiosa, and the dose in the spongiosa is reduced. Generally, the organ doses reported in Schlattl et al. (2007) correspond to the size-matched phantom data of PCXMC to within about 20%, and are sometimes lower and sometimes higher. For some organs the data (e.g., thyroid, skin, lungs, female liver and female thyroid) agree notably better, within about 5–10 % for energies above 20 keV. Typically, the doses in the two different-sized phantoms vary less in PCXMC than they do in the data of Schlattl et al. An example of typical organ data, the stomach, is shown in Figure 10.

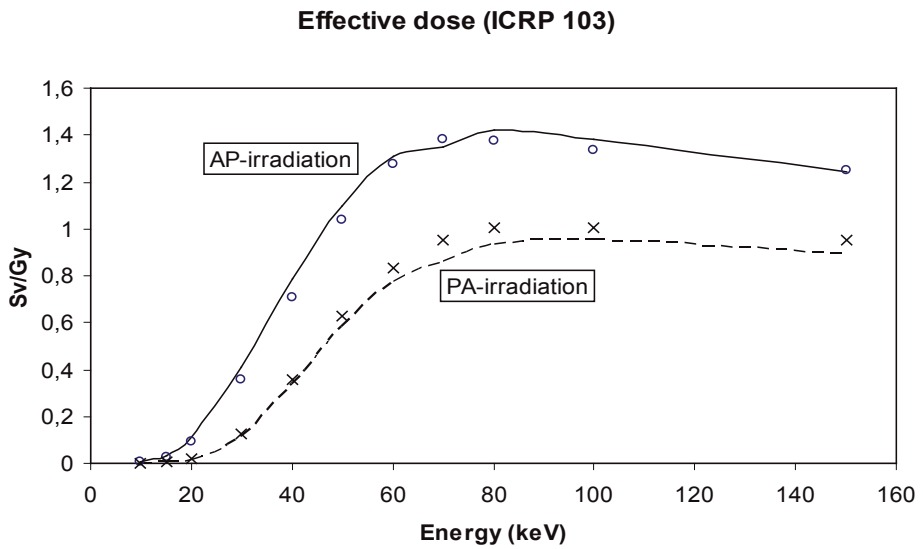

Figure 8. A comparison of the photon energy dependence of conversion factors from air kerma to effective dose. The data of Schlattl et al. (2007) are represented as curves and data points calculated with PCXMC 2.0 are marked with o and ×. Whole body irradiation of the phantoms with monochromatic and unidirectional photons. PCXMC data calculated as the average of doses in phantoms matched to the size of the reference phantoms of Schlattl et al.

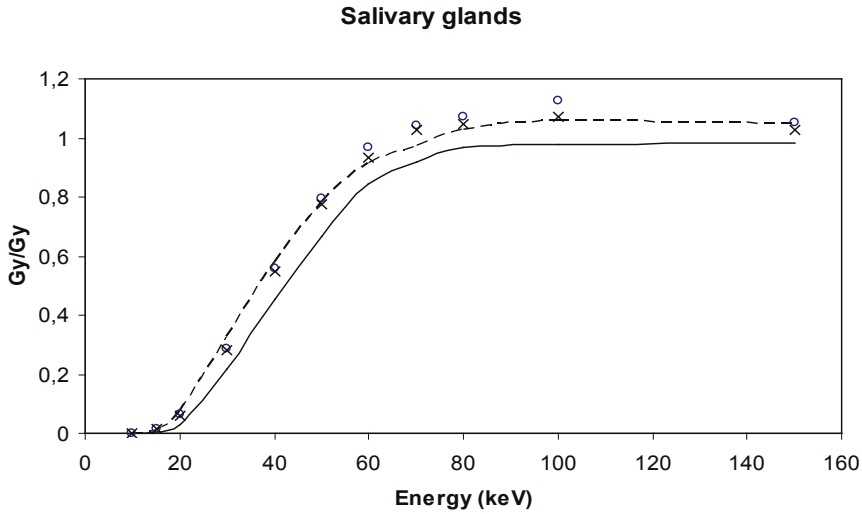

Figure 9. A comparison of the photon energy dependence of conversion factors from air kerma to the dose in salivary glands. Continuous curve: 'Regina' (Schlattl et al. 2007); points marked with o: PCXMC data for a phantom matched in size with 'Regina'. Broken curve: 'Rex' (Schlattl et al. 2007); points marked with ×: PCXMC data for a phantom matched in size with 'Rex'. Whole body AP irradiation of the phantoms with monochromatic, unidirectional photons.

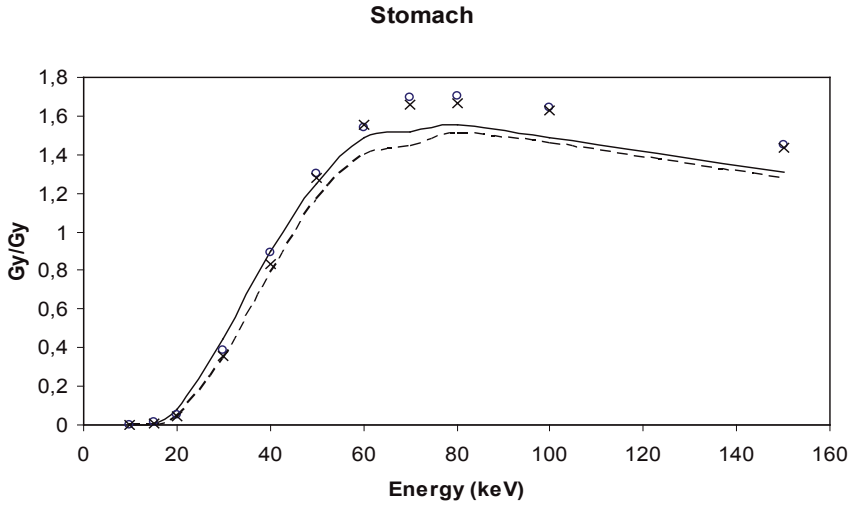

Figure 10. A comparison of the photon energy dependence of conversion factors from air kerma to the dose in the stomach. Continuous curve: 'Regina' (Schlattl et al. 2007); points marked with o: PCXMC data for a phantom matched in size with 'Regina'. Broken curve: 'Rex' (Schlattl et al. 2007); points marked with ×: PCXMC data for a phantom matched in size with 'Rex'. Whole body AP irradiation of the phantoms with monochromatic, unidirectional photons.

The usability of the phantom size modification feature of PCXMC has been demonstrated in an extreme case by Smans et al. (2008) who calculated doses in two premature babies with weights of 590 g and 1910 g. The differences between the results of PCXMC and the Monte Carlo software that was used in their work were explained by the differences in the phantom models and the difficulty to place an x-ray field similarly in different phantoms. The dose conversion values in that paper were made with PCXMC 1.5.2. We have repeated the calculations with PCXMC 2.0, and obtained essentially the same results as were reported in the paper of Smans et al. (2008); in this case the differences between the two PCXMC versions are caused mainly by the changes in the densities and composition of the phantom tissues. The data of Smans et al. (2008) and the newly calculated results for the chest AP examination of the smaller phantom are shown in Table V. In order to demonstrate the remarkable effect of field location in such comparisons, the table also includes PCXMC 2.0 data calculated with a slightly larger field and a downward displacement of the x-ray field by 0.5 cm.

Similar organ dose differences between computational and voxel phantoms have also been seen in the papers of Staton et al. (2003), Lee et al. (2006c) and Pazik et al. (2007); dose differences of the same order are obtained also in doses of different voxel phantoms (Zankl et al. 2002, Schlattl et al. 2007).

Table V. Comparison of the organ dose conversion data for a chest AP examination calculated by Smans et al (2008) with data calculated with PCXMC 2.0 for a premature baby of 590 g weight. The last column shows data calculated for the case of a slightly larger and slightly lower located x-ray field. X-ray tube voltage 65 kV, total filtration 4 mm Al, FSD 105 cm.

Organ or tissue	**Smans et al. (2008) 7×5 cm² field voxel phantom (Gy/Gy)**	**PCXMC 1.5 7×5 cm² field (Gy/Gy)**	**PCXMC 2.0 7×5 cm² field (Gy/Gy)**	**PCXMC 2.0 7×6 cm² field 0.5 cm lower (Gy/Gy)**
Active bone marrow	0.13	0.11	0.15	0.18
Adrenals	0.06	0.17	0.20	0.40
Brain	0.01	0.00	0.01	0.01
Colon	0.01	0.01	0.01	0.03
Heart	0.89	0.87	0.94	0.96
Kidneys	0.02	0.04	0.04	0.14
Liver	0.28	0.19	0.23	0.55
Lungs	0.95	0.82	0.82	0.84
Oesophagus	0.54	0.45	0.51	0.58
Pancreas	0.08	0.10	0.11	0.63
Skeleton	0.50	0.74	0.66	0.77
Skin	0.15	0.16	0.17	0.20
Small intestine	0.02	0.01	0.02	0.03
Spleen	0.47	0.11	0.13	0.45
Stomach	0.22	0.11	0.14	0.51
Testicles	0.00	0.00	0.00	0.00
Thymus	0.93	1.05	1.05	1.06
Thyroid	0.09	0.09	0.08	0.08
Urinary bladder	0.00	0.00	0.00	0.01

6 Risk assessment

Many mathematical models have been developed for estimating the cancer risk resulting from an exposure to ionising radiation. One such set of models is developed by the BEIR (Committee on the Biological Effects of Ionizing Radiations, BEIR 2006). The BEIR VII committee has derived risk models both for cancer incidence and for cancer mortality. The models take into account the cancer site, sex, age at the exposure and attained age. Presently, low dose rates and small doses are believed to yield a relatively lower cancer risk compared to high dose rates and large doses. This reduction in risk is accounted for by the dose and dose rate reduction factor (DDREF).

Age-dependent mortality rates are used for subsequent assessment of lifetime cancer risk. Risk models are presented for leukaemia, solid cancers in some organs and for all solid cancers combined. For all these cancer types the BEIR VII committee derived absolute and relative risk models: in the absolute risk model excess cancer risk from radiation is independent of the background cancer risk (i.e., cancers from other causes than radiation) and in the relative risk model the radiation risk is proportional to the background cancer risk. The BEIR VII committee combines these models in their final risk estimate.

Many factors, e.g., limitations in epidemiologic data for radiation-induced cancer, contribute to the uncertainty of risk estimation. The BEIR VII committee suggests that the risk estimates should be regarded with a healthy scepticism, placing more emphasis on the magnitude of the risk. The committee estimates that the excess cancer mortality due to radiation can be estimated within a factor of two (at 95% confidence level). For leukaemia the corresponding factor is four. For individual solid cancer sites the risk estimation may have large uncertainties, up to an order of magnitude or more (BEIR 2006).

For solid cancers the models of the excess relative and absolute risk (ERR and EAR, respectively) at attained age t are of the form (BEIR 2006)

$$\mathrm{ERR}(t,e,D) \text{ or } \mathrm{EAR}(t,e,D) = \beta_S D \exp\left(\gamma e^*\right)\left(t / 60\,\mathrm{a}\right)^{\eta} , \tag{6}$$

where e is age at exposure in years, $e^* = (e - 30\ \mathrm{a})/10\ \mathrm{a}$ when $e < 30$ a, and e^* is equal to zero for $e \geq 30$ a for other solid cancers than breast cancer and thyroid cancer. For these two cancers, $e^* = (e - 30\ \mathrm{a})/10\ \mathrm{a}$ for all values of e.[3)] Attained age (in years) is t, and D is the organ or tissue equivalent dose. β_S, γ and η are fitting parameters of the model. For leukaemia the ERR and EAR models are of the form

[3)] This difference of the risk models of the female breast and the thyroid from the risk models of other organs was not properly taken into account in PCXMC version 2.0.0. It has been corrected in version 2.0.1.

$$\mathrm{ERR}(t,e,D) \text{ or } \mathrm{EAR}(t,e,D) = \beta_S D(1+\theta D) \cdot \exp\left[\gamma e^* + \delta \log\left((t-e)/25\,\mathrm{a}\right) + \varphi e^* \log\left((t-e)/25\,\mathrm{a}\right)\right] \quad (7)$$

where t - e is the time elapsed after the exposure and D is the equivalent dose in bone marrow. θ , δ and φ are fitting parameters. The site-specific EAR values in the BEIR VII model consider cancer incidence. Therefore, in order to estimate cancer mortality, the incidence values are scaled with the ratio of the sex- and age-specific mortality and incidence rates for the site-specific cancer in question (BEIR 2006).

BEIR (2006) does not provide risk estimates for all organs and tissues. The risk of cancer death from other solid cancers than in those organs that are included in the risk models is estimated in PCXMC using BEIR's model for "other solid cancers". The related cancer statistics is taken as the statistics for all solid cancers from which the separately considered solid cancer types have been subtracted. It is not self-evident how the dose corresponding to these "other solid cancers" should be determined when the dose distribution in the body is not uniform. If one would use the average dose of all the organs involved, this dose would correspond mainly to the dose in muscle tissue because of its large mass, and this would presumably be not reasonable. In PCXMC, therefore, a weighted average dose in the other organs and tissues ("weighted remainder") has been used. This weighted average dose used in the risk estimation of "other solid cancers" is calculated as the weighted average dose in organs and tissues that are not given a direct risk estimate. The weighting is done with the tissue weighting factors of ICRP Publication 103, renormalized such that their sum is equal to one. In effect, this involves the assumption that the relative sensitivities of these organs are in proportion to the tissue weighting factors of ICRP 103.

The cancer risks are non-zero only after a latency period. The BEIR VII committee assumes that solid cancers have a latency period of 5 years. For leukaemia the latency period is 2 years. These values are used in PCXMC as a default.

The excess risk values are the basis of the lifetime risk estimates. The lifetime risks can be assessed with various quantities. PCXMC uses three different quantities:

- Risk of exposure-induced death (REID)
- Loss of life expectancy (LLE)
- Loss of life expectancy per radiation induced fatal cancer (LLE/REID).

The definitions of these quantities are (Thomas et al. 1992)

$$\mathrm{REID}_c(e,D) = \int_{\tau}^{\infty} \left[\mu_c(t \mid e,D) - \mu_c(t)\right] S(t \mid e,D)\,dt \tag{8}$$

and

$$\mathrm{LLE}(e,D) = \int_{\tau}^{\infty} S(t \mid e)\,dt - \int_{\tau}^{\infty} S(t \mid e,D)\,dt. \tag{9}$$

Here, $\mu_c(t \mid e, D)$ is the mortality rate at age t due to death cause c, given that the subject was alive at the age of exposure e and the corresponding dose at that age was D. In the excess relative risk model

$$\mu_c(t \mid e,D) = \left[1 + \mathrm{ERR}_c(t,e,D)\right]\mu_c(t), \tag{10}$$

where $\mu_c(t)$ is the background mortality rate related to the death cause c. In the excess absolute risk model

$$\mu_c(t \mid e,D) = \mathrm{EAR}_c(t,e,D) + \mu_c(t). \tag{11}$$

$S(t \mid e, D)$ is the conditional probability that the subject is alive at age t, given a dose D at the age e. For an unexposed subject the probability of surviving to age t is $S(t \mid e)$. These conditional survival functions are calculated from mortality statistics, cancer mortality rates and, for $S(t \mid e, D)$, the risk models. Specifically,

$$S(t \mid e,D) = \exp\left[-\int_{e}^{t} \mu(x \mid e,D)\,dx\right], \tag{12}$$

where $\mu(t \mid e, D)$ is the death rate for all causes combined. Thus, the software accounts for the reduction in S caused by the radiation exposure, and the site-specific REID estimates for different cancers can be added. The sum obtained reflects the total risk from the exposure in question. The lower limit in the integrals (8) and (9) is $\tau = e + \lambda$, where λ is the latency period in years. In PCXMC, the upper integration limit has been set to 120 years instead of infinity in these equations.

The concept of REID originates from cohort analysis techniques: death rates in the exposed and in the unexposed cohorts are compared. A null hypothesis corresponds to a statistically negligible difference between the two groups. A positive REID value indicates excess deaths in the exposed cohort.

In the risk assessment model of BEIR the REID-values of relative and absolute risk models are combined and they are given the weights of 0.7 and 0.3, respectively [the weighting is done on a logarithmic scale as suggested by BEIR (2006)]. For the lung cancer these weights are reversed. For the breast cancer

only the absolute model is used and for the thyroid cancer only the relative risk model is used. The DDREF division is done after the weighting.

The loss of life expectancy (LLE) is the difference between the expectation of life for a person exposed at age *e* and of an unexposed person who was alive at that age. LLE/REID describes the average length of life lost per excess cancer death. More information on the quantities can be found in Thomas et al. (1992) and Vaeth and Pierce (1990). These quantities have not been considered in BEIR (2006). Therefore, PCXMC estimates LLE using the relative risk model only and does not use the DDREF concept in calculating it.

The BEIR VII -committee simplified the definition of REID by replacing $S(t \mid e, D)$ by $S(t \mid e)$. The resulting risk estimate was called the lifetime attributable risk (LAR) (BEIR 2006). Also, the concept of excess lifetime risk (ELR) is sometimes used in the literature. For practical purposes, at typical dose levels encountered in x-ray diagnostics, REID, ELR and LAR can be interpreted to present the excess radiation-induced cancer risk. Their numerical values are close enough to be interpreted identical considering the uncertainties involved in the models.

The BEIR VII -committee recommends to use the dose and dose rate reduction factor value DDREF = 1.5 for solid cancers and DDREF = 1 for leukaemia. As a default, these values are used also in PCXMC. If the equivalent doses are large (several tens or hundreds of mSv), the risk estimates should be regarded with care: it might be more appropriate to use DDREF = 1 also for solid cancers in such cases. This can be achieved by multiplying the solid cancer REID estimates of PCXMC by 1.5. Moreover, the risk models describe only the stochastic effects of ionising radiation – if deterministic effects are possible, the risk estimates should be interpreted carefully.

The necessary input data for the calculation include the sex-specific mortality and cancer incidence rates. In the default data sets in PCXMC these data are mostly given in five year intervals and are assumed to be constant within the age intervals. The Finnish mortality data are from Statistics Finland databank (www.tilastokeskus.fi) and the cancer mortality and incidence data are from Finnish Cancer Registry (www.cancerregistry.fi), retrieved on March 20, 2007. The Euro-American and Asian mortality and cancer incidence data are from ICRP publication 103 (ICRP, 2007). Chronic lymphocytic leukaemia is believed to be unrelated to radiation exposure. Therefore it is excluded from the ICRP 103 leukaemia mortality data. The Finnish mortality and incidence data include all leukaemia types, leading to a slightly overestimated leukaemia risk. This overestimation is much less than the uncertainty present in the risk model for leukaemia.

Mortality statistics for Euro-American males (ICRP 2007) are illustrated in Figure 11. Examples of risk calculations for females are shown in Tables VI and VII. The values from BEIR (2006), Table 12D-2, are in reasonable agreement with the data calculated using PCXMC with American cancer data (retrieved from seer.cancer.gov) and Euro-American mortality data (ICRP 2007). Therefore, the implementation of the risk model of BEIR in PCXMC can be considered valid. The differences between the REID values calculated with PCXMC (for other regional statistics) and those in BEIR (2006) just reflect the differences in the regional mortality and cancer statistics used in PCXMC and the American data used in BEIR (2006).

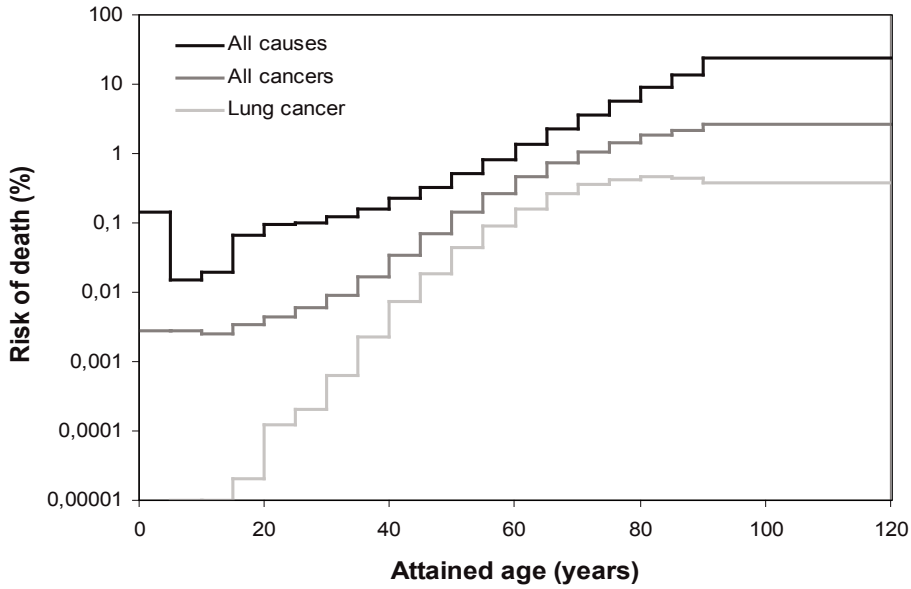

Figure 11. Risks of death (in percent per year) for Euro-American males (ICRP 2007). Risks of death for all causes combined (black line), for all cancers combined (grey line) and for lung cancer (light grey line) are shown for five year age intervals. The highest age group covers ages 90–120 years.

Table VI. The excess number of deaths per 10^5 females assuming various mortality statistics. A single dose of 0.1 Gy to stomach is assumed. The risk estimates have been adjusted by a DDREF of 1.5. The BEIR VII values (second column) are from Table 12D-2 of BEIR (2006). The American data (third column) were calculated with PCXMC using American cancer mortality data, retrieved from seer.cancer.gov (not included in the PCXMC distribution), and Euro-American mortality statistics from the ICRP publication 103. These data are presented here in order to compare PCXMC-calculated data with those given in BEIR VII. The last three columns use mortality and cancer statistics which are readily included in the data files of PCXMC.

	Number of excess deaths				
Age at exposure (years)	**BEIR VII**	**American statistics (PCXMC)**	**Asian statistics (PCXMC)**	**Euro-American statistics (PCXMC)**	**Finnish statistics (PCXMC)**
0	57	61	166	83	104
10	41	44	119	60	74
20	29	31	85	43	54
30	21	22	60	30	38
40	20	21	57	30	37
50	19	20	54	28	35
60	16	18	47	26	31
70	13	15	38	22	25
80	8	11	24	16	17

Table VII. The excess number of deaths per 10^5 females assuming various mortality statistics. A single dose of 0.1 Gy to breasts is assumed. The risk estimates have been adjusted by a DDREF of 1.5. The BEIR VII values are from Table 12D-2 of BEIR (2006). The American data (third column) were calculated with PCXMC using American cancer mortality data, retrieved from seer.cancer.gov (not included in the PCXMC distribution), and Euro-American mortality statistics from the ICRP publication 103. These data are presented here in order to compare PCXMC-calculated data with those given in BEIR VII. The last three columns use mortality and cancer statistics which are readily included in the data files of PCXMC.

	Number of excess deaths				
Age at exposure (years)	**BEIR VII**	**American statistics (PCXMC)**	**Asian statistics (PCXMC)**	**Euro-American statistics (PCXMC)**	**Finnish statistics (PCXMC)**
0	274	287	338	363	302
10	167	173	203	219	182
20	101	104	122	132	109
30	61	62	73	79	66
40	35	36	43	46	39
50	19	20	24	26	22
60	9	11	12	14	12
70	5	5	6	7	6
80	2	3	4	3	3

References

Almén A and Mattsson S. On the calculation of effective dose to children and adolescents. J. Radiol. Prot. 1996; 16: 81–89.

Andreo P. Monte Carlo techniques in medical radiation physics. Phys. Med. Biol. 1991; 36: 861–920.

BEIR–Committee on the Biological Effects of Ionizing Radiations. Health effects of exposure to low levels of ionizing radiation. BEIR V. Washington, D.C: National Academy of Sciences; 1990.

BEIR–Committee to Assess Health Risks from Exposure to Low Levels of Ionizing Radiation. Health Risks from Exposure to Low Levels of Ionizing Radiation. BEIR VII. Washington D.C: National Academy of Sciences; 2006.

Birch R and Marshall M. Computation of bremsstrahlung x-ray spectra and comparison with spectra measured with a Ge(Li) detector. Phys. Med. Biol. 1979; 24: 505–517.

Bouchet LG, Bolch WE, Weber DA, Atkins HL and Poston JW. MIRD Pamphlet No 15: Radionuclide S values in a revised dosimetric model of the adult head and brain. J. Nucl. Med. 1999; 40(3): 62S–101S.

Büermann L, Grosswendt B, Kramer H-M, Selbach H-J, Gerlach M, Hofmann M, Krumrey M. Measurement of the x-ray mass energy-absorption coefficient of air using 3 keV to 10 keV synchrotron radiation. Phys. Med. Biol. 2006; 51: 5125–5150.

Cristy M. Mathematical phantoms representing children of various ages for use in estimates of internal dose, NUREG/CR-1159, ORNL/NUREG/TM-367. Oak Ridge: Oak Ridge National Laboratory; 1980.

Cristy M and Eckerman KF. Specific absorbed fractions of energy at various ages from internal photon sources. I. Methods. Report ORNL/TM-8381/V1. Oak Ridge: Oak Ridge National Laboratory; 1987.

Drexler G, Panzer W, Widenmann L, Williams G and Zankl M. The calculation of dose from external photon exposures using reference human phantoms and

Monte Carlo methods, Part III: Organ doses in x-ray diagnosis. GSF-Bericht 11/90. Neuherberg: GSF; 1990.

Drexler G, Panzer W, Petoussi N and Zankl M. 1993 Effective dose – how effective for patients? Radiat. Environ. Biophys. 32, 209–219.

Grosswendt B. Dependence of the photon backscatter factor for water on source-to-phantom distance and irradiation field size, Phys. Med. Biol. 1990; 35: 1233–1245.

Eckerman KF and Ryman JC. External exposure to radionuclides in air, water, and soil. Federal Guidance Report No. 12, Report EPA-402-R-93-081. Oak Ridge: Oak Ridge National Laboratory; 1993.

Eckerman KF, Cristy M and Ryman JC. The ORNL mathematical phantom series. Manuscript available from the internet at http://homer.ornl.gov/vlab/mird2.pdf ;1996.

Hart D, Jones DG and Wall BF. Estimation of effective dose in diagnostic radiology from entrance surface dose and dose-area product measurements, Report NRPB-R262. London: HMSO; 1994a.

Hart D, Jones DG and Wall BF. Normalised organ doses for medical x-ray examinations calculated using Monte Carlo techniques, NRPB-SR262. Chilton: NRPB; 1994b.

Hart D, Jones DG and Wall BF. Coefficients for estimating effective doses from paediatric x-ray examinations, Report NRPB-R279. London: HMSO; 1996a.

Hart D, Jones DG and Wall BF. Normalised organ doses for paediatric x-ray examinations calculated using Monte Carlo techniques, NRPB-SR279. Chilton: NRPB; 1996b.

Hart D and Wall BF. Radiation exposure of the UK population from medical and dental X-ray examinations, NRPB-W4. Chilton: NRPB; 2002.

Helmrot E, Petterson H, Sandborg M and Altén JN. Estimation of dose to the unborn child at diagnostic X-ray examinations based on data registered in RIS/PACS. Eur. Radiol. 2007; 17: 205–209.

Hubbel JH, Veigele WJ, Briggs EA, Brown RT, Cromer DT and Howerton RJ. Atomic form factors, incoherent scattering functions and photon scattering cross sections. J. Phys. Chem. Ref. Data 1975;4: 471–538.

ICRP–International Commission on Radiological Protection. 1990 Recommendations of the International Commission on Radiological Protection, ICRP Publication 60. Annals of the ICRP 1991; 21 (1–3).

ICRP–International Commission on Radiological Protection. Age-dependent doses to members of the public from intake of radionuclides: Part 4, Inhalation dose coefficients. ICRP Publication 71. Annals of the ICRP 1995; 25 (3–4).

ICRP–International Commission on Radiological Protection. Radiological Protection and Safety in Medicine. ICRP Publication 73. Annals of the ICRP 1996; 26.

ICRP–International Commission on Radiological Protection. Basic anatomical and physiological data for use in radiological protection: reference values. ICRP Publication 89. Annals of the ICRP 2002; 32 (3–4).

ICRP–International Commission on Radiological Protection. The 2007 Recommendations of the International Commission on Radiological Protection. ICRP Publication 103. Annals of the ICRP 2007; 37 (2–4).

ICRU–International Commission on Radiation Units and Measurements. Phantoms and computational models in therapy, diagnosis and protection. ICRU Report 48. Bethesda: International Commission on Radiation Units and Measurements; 1992a.

ICRU–International Commission on Radiation Units and Measurements. Measurement of dose equivalents from external photon and electron radiations. ICRU Report 47. Bethesda: International Commission on Radiation Units and Measurements; 1992b.

ICRU–International Commission on Radiation Units and Measurements. Patient Dosimetry for X Rays Used in Medical Imaging. ICRU Report 74. Journal of the ICRU 2005; 5 (2).

Jones DG and Wall BF. Organ doses from medical x-ray examinations calculated using Monte Carlo techniques, NRPB -R186. London: HMSO; 1985.

Kerr GD and Eckerman KF. Neutron and photon fluence-to-dose conversion factors for active marrow of the skeleton. In: Schraube H, Burger G, and Booz J. (eds). Proceedings of the fifth symposium on neutron dosimetry, Volume I, Radiation protection aspects. EUR 9762 EN. Luxembourg: CEC; 1985.

King SD and Spiers FW. Photoelectron enhancement of the absorbed dose from X rays to human bone marrow: experimental and theoretical studies. Br. J. Radiol. 1985; 58: 345–356.

Kramer R, Zankl M, Williams G and Drexler G. The calculation of dose from external photon exposures using reference human phantoms and Monte Carlo methods, Part I: The male (Adam) and female (Eva) adult mathematical phantoms. GSF-Bericht S-885, reprinted 1986. München: Gesellschaft fur Strahlen- und Umweltforschung mbH; 1982.

Kramer R, Khoury HJ and Vieira JW. CALDose_X – a software tool for the assessment of organ and tissue absorbed doses, effective dose and cancer risks in diagnostic radiology. Available from http://www.grupodoin.com/ing.html; 2008.

Lee C, Lee C, Williams JL and Bolch WE. Whole-body voxel phantoms of paediatric patients–UF Series B. Phys. Med. Biol. 2006a; 51: 4649–4661.

Lee C, Lee C, Shah AP and Bolch WE. An assessment of bone marrow and bone endosteum dosimetry methods for photon sources. Phys. Med. Biol. 2006b; 51: 5391–5407.

Lee C, Lee C and Bolch WE. Age-dependent organ and effective dose coefficients for external photons: a comparison of stylized and voxel-based paediatric phantoms. Phys. Med. Biol. 2006c; 51: 4663–4688.

Martin CJ. Effective dose: how should it be applied to medical exposures? Br. J. Radiol. 2007; 80: 639–647.

McMaster WH, Kerr, Del Grande B, Mallet JH, and Hubbell IH. Compilation of X-ray cross-sections, Report UCRL-50174 Sec 2, Rev 1. Springfield: NTIS; 1969.

Möller TB and Reif E. Pocket atlas of cross-sectional anatomy. Computed tomography and magnetic resonance imaging. Volume 1: Head, neck, spine and joints. Stuttgart: Georg Thieme Verlag; 1994a.

Möller TB and Reif E. Pocket atlas of cross-sectional anatomy. Computed tomography and magnetic resonance imaging. Volume 2: Thorax, abdomen and pelvis. Stuttgart: Georg Thieme Verlag; 1994b.

Pazik FD, Staton RJ, Williams JL, Arreola MM, Hintenlang DE and Bolch WE. Organ and effective doses in newborns and infants undergoing voiding cystourethrograms (VCUG): A comparison of stylized and tomographic phantoms. Med. Phys. 2007; 34: 294–306.

Petoussi-Henss N, Zankl M, Drexler G, Panzer W and Regulla D. Calculation of backscatter factors for diagnostic radiology using Monte Carlo methods. Phys. Med.Biol. 1998; 43: 2237–2250.

Qatarneh SM, Kiricuta I-C, Brahme A, Tiede U and Lind BK. Three-dimensional atlas of lymph node topography based on the visible human data set. The Anatomical Record (Part B: new anat.) 2006; 289B: 98–111.

Rosenstein M . Organ doses in diagnostic radiology, Publication (FDA) 76-8030. Washington D.C: U.S. Government Printing Office; 1976a.

Rosenstein M. Handbook of selected organ doses for projections common in diagnostic radiology. FDA Publication 76-8031. Rockville, MD: HEW; 1976b.

Rosenstein M, Beck TJ and Warner GG. Handbook of selected tissue doses for projections common in pediatric radiology. HEW Publication FDA 79-8079. Washington D.C: U.S. Government Printing Office; 1979.

Rosenstein M, Suleiman OH, Burkhart RL, Stern SH and Williams G. Handbook of selected tissue doses for the upper gastrointestinal fluoroscopic examination. HHS Publication FDA 92-8282. Rockville, MD: HHS; 1992.

Scanff P, Donadieu J, Pirard P and Aubert B. Population exposure to ionizing radiation from medical examinations in France. Br. J. Radiol. 2008; 81: 204–213.

Schlattl H, Zankl M and Petoussi-Henss N. Organ dose conversion coefficients for voxel models of the reference male and female from idealized photon exposures. Phys. Med. Biol. 2007; 52: 2123–2145.

Schmidt PWE, Dance DR, Skinner CL, Castellano Smith IA and McNeill JG. Conversion factors for the estimation of effective dose in paediatric cardiac angiography. Phys. Med. Biol. 2000; 45: 3095–3107.

Schultz FW, Geleijns J, Spoelstra FM and Zoetelief J. Monte Carlo calculations for assessment of radiation dose to patients with congenital heart defects and to staff during cardiac catheterizations. Br. J. Radiol. 2003; 76: 638–647.

Smans K, Tapiovaara M, Cannie M, Struelens L, Vanhavere F, Smet M and Bosmans H. Calculation of organ doses in x-ray examinations of premature babies. Med. Phys. 2008; 35 (2): 556–568.

Staton RJ, Pazik FD, Nipper JC, Williams JL and Bolch WE. A comparison of newborn stylized and tomographic models for dose assessment in paediatric radiology. Phys. Med. Biol. 2003; 48: 805–820.

Stern SH, Rosenstein M, Renaud L, and Zankl M. Handbook on selected tissue doses for fluoroscopic and cineangiographic examination of the coronary arteries. HHS Publication FDA 95-8289. Rockville, MD: CDRH; 1995.

Stokell PJ, Robb JD, Crick MJ and Muirhead CR. SPIDER 1 Software for evaluating the detriment associated with radiation exposure. NRPB -R261. London: HMSO; 1993.

Storm E and Israel HI. Photon cross sections from 1 keV to 100 MeV for elements Z=1 to Z=100. Nuclear Data Tables, Sect A 1970; 7: 565–688.

Tapiovaara M, Lakkisto M And Servomaa A. PCXMC: A PC-based Monte Carlo program for calculating patient doses in medical x-ray examinations. Report STUK-A139. Helsinki: Finnish Centre for Radiation and Nuclear Safety; 1997.

Thomas D, Darby S, Fagnani F, Hubert P, Vaeth M and Weiss K. Definition and estimation of lifetime detriment from radiation exposures: Principles and methods. Health Physics 1992; 63(3): 259–272.

UNSCEAR–United Nations Scientific Committee on the Effects of Atomic Radiation. Sources and effects of ionising radiation. Vol. I, Sources, Annex D, Medical radiation exposures. New York: United Nations; 2000.

Vattulainen I, Kankaala K, Saarinen J and Ala-Nissilä T. Pseudosatunnaislukugeneraattorien ominaisuuksien vertailu. CSC Research Reports R05/92. Helsinki:Yliopistopaino; 1993.

Vaeth M and Pierce DA. Calculating Excess Lifetime Risk in Relative Risk Models. Environmental Health Perspectives 1990; 87: 83–94.

Zankl M, Petoussi N, Veit R, Drexler G and Fendel H. Organ doses for a child in diagnostic radiology: comparison of a realistic and a MIRD-type phantom. In: Moores BM, Wall BF, Eriskat H and Schibilla H (eds.) Optimization of image quality and patient exposure in diagnostic radiology. BIR Report 20. London: British Institute of Radiology; 1989. pp. 196–198.

Zankl M, Fill U, Petoussi-Henss N and Regulla D. Organ dose conversion coefficients for external photon irradiation of male and female voxel models. Phys. Med. Biol. 2002; 47: 2367–2385.

STUK-A reports/STUK-A-sarjan julkaisuja

STUK-A231 Tapiovaara M, Siiskonen T. PCXMC, A Monte Carlo program for calculating patient doses in medical x-ray examinations. Helsinki 2008

STUK-A230 Salomaa S, Sirkka L. (toim.), Tutkimushankkeet 2006-2008. Helsinki 2008

STUK-A229 Arvela H, Reisbacka H. Asuntojen radonkorjaaminen. Helsinki 2008

STUK-A228 Toivonen H, Lahtinen J, Pöllänen R (toim.). Säteilyyn liittyvät uhkakuvat - Ydinvoimalaturma. Helsinki 2008

STUK-A227 Ilus E, Klemola S, Vartti V-P, Mattila J, Ikäheimonen T. K. Monitoring of radionuclides in the vicinities of Finnish nuclear power plants in 2002–2004. Helsinki 2008

STUK-A226 Sinkko K, Ammann M, Hämäläinen RP, Mustajoki J. Facilitated workshop - a participatory method for planning of countermeasures in case of a nuclear accident. Helsinki 2008.

STUK-A225 Vesterbacka P, Turtiainen T, Hämäläinen K, Salonen L, Arvela H. Metoder för avlägsnande av radionuklider från hushållsvatten. Helsinki 2008.

STUK-A224 Kuukankorpi S, Toivonen H, Moring M, Smolander P. Mobile Spectrometry System for Source Finding and Prompt Reporting. Helsinki 2007.

STUK-A223 Jussila P. Thermomechanics of swelling unsaturated porous media. Compacted bentonite clay in spent fuel disposal. Helsinki 2007.

STUK-A222 Hutri K-L. An approach to palaeoseismicity in the Olkiluoto (sea) area during the early Holocene. Helsinki 2007.

STUK-A221 Valmari T, Arvela H, Reisbacka H. Päiväkotien radonkartoitus. Helsinki 2007.

STUK-A220 Karppinen J, Järvinen H. Tietokonetomografialaitteiden käytön optimointi. Helsinki 2006.

STUK-A219 Tapiovaara M. Relationships between physical measuments and user evaluation of image quality in medical radiology – a review. Helsinki 2006.

STUK-A218 Ikäheimonen TK, Klemola S, Ilus E, Varti V-P, Mattila J. Monitoring or radionuclides in the vicinities of Finnish nuclear power plants in 1999–2001. Helsinki 2006.

STUK-A217 Ikäheimonen TK (toim.). Ympäristön radioaktiivisuus Suomessa – 20 vuotta Tshernobylista. Symposium Helsingissä 25.–26.4.2006. Helsinki 2006.

STUK-A216 Pastila R. Effect of long-wave UV radiation on mouse melanoma: An in vitro and in vivo study. Helsinki 2006.

STUK-A215 Rantavaara A. Elintarvikeketjun suojaustoimenpiteet laskeumatilanteiden varalle. Helsinki 2005.

STUK-A214 Sinkko K, Ammann M, Hämäläinen RP, Mustajoki J. Facilitated workshop on clean-up actions in inhabited areas in Finland after an accidental release of radionuclides. Helsinki 2005.

STUK-A213 Vesterbacka P. ^{238}U-series radionuclides in Finnish groundwater-based drinking water and effective doses. Helsinki 2005.

STUK-A212 Kantala T. Elintarviketeollisuuslaitosten ja niiden ympäristön puhdistustoimenpiteet säteilytilanteessa. Helsinki 2005.

STUK-A211 Muikku M, Arvela H, Järvinen H, Korpela H, Kostiainen E, Mäkeläinen I, Vartiainen E, Vesterbacka K. Annoskakku 2004 – suomalaisten keskimääräinen efektiivinen annos. Helsinki 2005.

STUK-A210 Salomaa S, Ikäheimonen TK (eds.). Research activities of STUK 2000–2004. Helsinki 2005.

STUK-A209 Valmari T, Rantavaara A, Hänninen R. Radioaktiivisten aineiden siirtyminen päästöpilven kulkeutumisen aikana tuotettaviin elintarvikkeisiin. Helsinki 2004.

STUK-A208 Kiuru A. Molecular biology methods in assessing radiation-induced hereditary risks in humans. Helsinki 2004.

STUK-A207 Sinkko K. Nuclear emergency response planning based on participatory decision analytic approaches. Helsinki 2004.

STUK-A206 Hämäläinen K, Vesterbacka P, Mäkeläinen I, Arvela H. Vesilaitosten vedenkäsittelyn vaikutus luonnon radionuklidipitoisuuksiin (VEERA). Helsinki 2004.

STUK-A205 Klemola S, Ilus E, Ikäheimonen TK. Monitoring of radionuclides in the vicinities of Finnish nuclear power plants in 1997 and 1998. Helsinki 2004.

A full list of publications is available from

Radiation and Nuclear Safety Authority (STUK)
P.O.Box 14
FI-00881 HELSINKI, FINLAND
Phone +358 9 759 881